

Department of Physics
Institute for Theoretical Physics
University of Tübingen, Germany
Master Degree in Astro & Particle Physics
Academic Year 2024-2025
August 1, 2025

Master's Thesis

Towards a twist-3 factorization of semi-inclusive deep inelastic scattering at NLO accuracy

Supervisor:
Prof. Marc Schlegel

Student:
Diego Scantamburlo

Co-supervisor:
Prof. Werner Vogelsang

...

Contents

1	Semi-inclusive deep inelastic scattering at next-to-leading-order	1
1.1	Leading-twist case	1
1.1.1	Virtual corrections	1
1.1.2	Real corrections	5
1.2	Transverse nucleon spin	9
1.2.1	Virtual graphs	10
1.2.2	Real graphs	11

Chapter 1

Semi-inclusive deep inelastic scattering at next-to-leading-order

We perform our pQCD calculation at next-to-leading order in dimensional regularization in $d = 4 - 2\epsilon$ dimensions. When it comes to renormalization, we adopt the common choice of using the minimal subtraction scheme ($\overline{\text{MS}}$).

1.1 Leading-twist case

1.1.1 Virtual corrections

The virtual graphs contributing at twist-2 level are shown in Fig.1.1 Since we are performing our pQCD calculation in light-cone gauge, we shall employ an appropriate technique to evaluate loop integrals that allows us to treat the denominator of the gluon propagator in this gauge. Notoriously, this $(r \cdot m)^{-1}$ term requires a careful treatment since it may lead to additional well-known *light-cone divergences*, i.e. when $r \cdot m \rightarrow 0$. Not surprisingly, it turns out that a light-cone decomposition of the loop momentum allows for a systematic procedure to integrate out the $+$, $-$ and perpendicular components. Since this technique is essential for calculating virtual corrections also at the twist-3 level, we present it here in detail for the simpler leading-twist case. The method

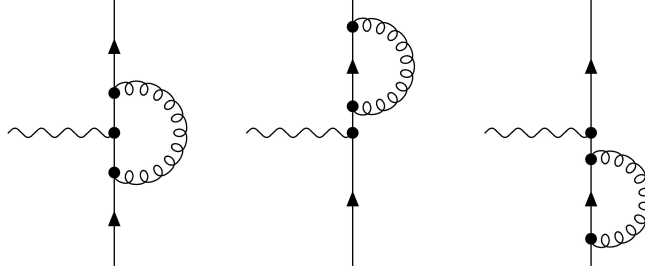


Figure 1.1: Virtual diagrams contributing to the leading-twist unpolarized cross section at NLO.

is quite general and can be readily extended to higher-twist contributions. Let's start by calculating the vertex correction graph. The amplitude reads

$$(\hat{\mathcal{M}}_{\text{NLO,vir}}^{q \rightarrow q})_{ij,ac}^\mu = \int \frac{d^d r}{(2\pi)^d} \frac{\tilde{N}_{ij,ac}^\mu(r)}{[(p-r)^2 + i\delta][(k-r)^2 + i\delta][r^2 + i\delta]r \cdot m}, \quad (1.1)$$

$$\tilde{N}_{ij,ac}^\mu(r) \equiv -ig_S^2 \mu^{4-d} T_{ab}^\alpha T_{bc}^\beta \delta_{\alpha\beta} [\gamma^\lambda (\not{p} - \not{r}) \gamma^\mu (\not{k} - \not{r}) \gamma^\eta]_{ij} [(r \cdot m) g_{\lambda\eta} - \kappa r_{(\lambda} m_{\eta)}].$$

As already anticipated, it is convenient to express the loop momentum in its light-cone decomposition $r^\mu = \alpha P_h^\mu + \beta m^\mu + r_\perp^\mu$ with $\alpha \equiv r \cdot m$ and $\beta \equiv r \cdot P_h$. By doing this, given a generic momentum p_j , the denominator of the propagators become of the form

$$(p_j - r)^2 + i\delta = (2\alpha - 2p_j \cdot m)(\beta - \beta_j), \quad \beta_j \equiv -\frac{r_\perp^2 + p_j^2 - 2\alpha p_j \cdot P_h + i\delta}{2\alpha - 2p_j \cdot m} \quad (1.2)$$

In order to simplify the calculation, we find that it is convenient to perform the integration at the level of the hadronic tensor, and not just the amplitude alone. This is because many terms that are present in the hard scattering amplitude $\hat{\mathcal{M}}$ may vanish when traced with correlators and the LO interfering amplitude. We have then

$$(W_{\text{NLO,vir}}^{q \rightarrow q})^{\mu\nu} = \int_{-\infty}^{+\infty} \frac{d\alpha}{2\pi} \frac{1}{2\alpha(2\alpha - 2p \cdot m)(2\alpha - 2k \cdot m)\alpha} \int \frac{d^{d-2} r_\perp}{(2\pi)^{d-2}} \\ \times \int_{-\infty}^{+\infty} \frac{d\beta}{2\pi} \frac{N^{\mu\nu}(\alpha, r_\perp, \beta)}{(\beta - \beta_0)(\beta - \beta_1)(\beta - \beta_2)}, \quad (1.3)$$

$$N^{\mu\nu} \equiv \frac{e_a^2 2x_B z_h}{Q^2} z_h^{-2\epsilon} \text{Tr} [\tilde{N}^\mu \Phi^a \gamma^\nu \Delta^a].$$

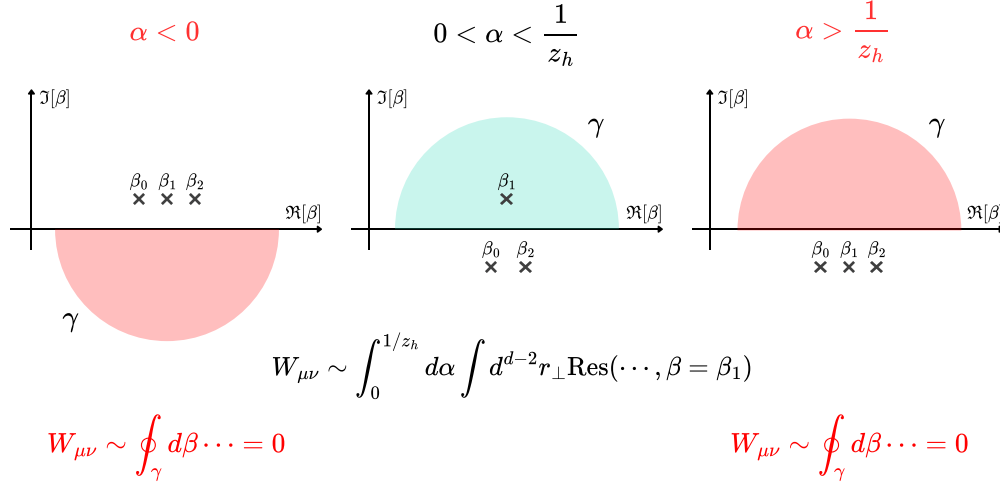


Figure 1.2: Sketch of the light-cone contour integration technique used for calculating virtual graphs in this work. Poles placements are studied and non-vanishing contributions to the hadronic tensor are identified with the residue theorem.

By studying the position of the poles β_j ($j = 0, 1, 2$) in the complex plane, we can use contour integration and the residue theorem to evaluate the β integral in a straightforward manner. In order to perform the integration in this way, the integrand should fall off at least as $\sim 1/\beta$ for large β (meaning that $N^{\mu\nu}$ should be at most quadratic in β , which turns out to be the case). Evidently, the poles β_j depend on α , as seen in Eq. (1.2). In particular, the pole will lay above or below the real axis depending on the sign of $2\alpha - 2p_j \cdot m$. By studying the imaginary part of all poles we can conveniently close the contour above or below the real axis and obtain the non-vanishing contributions to the β integral. This, in turn, restricts the domain of integration over α , since for certain values of α all the poles lie above (below) the real axis and we can close the contour below (above) and obtain zero since the curve does not include any poles. Going back to the integral above, we find that it is non-vanishing only for $0 < \alpha < 1/z_h$, and the only relevant pole is $\beta_1 = -(r_{\perp}^2 + i\delta)/2(\alpha - 1/z_h)$. A graphical sketch of the contour integration procedure can be found in Fig. 1.2. We then have

$$(W_{\text{NLO,vir}}^{q \rightarrow q})^{\mu\nu} = \int_0^{1/z_h} \frac{d\alpha}{2\pi} \frac{1}{2\alpha(2\alpha - 2p \cdot m)(2\alpha - 2k \cdot m)\alpha} \int \frac{d^{d-2}r_\perp}{(2\pi)^{d-2}} \times 2\pi i \text{Res} \left[\frac{N^{\mu\nu}(\alpha, r_\perp, \beta)}{2\pi(\beta - \beta_0)(\beta - \beta_1)(\beta - \beta_2)}, \beta = \beta_1 \right] \quad (1.4)$$

After β contour integration, the denominator factors arrange as $\beta_1 - \beta_j = C_{1j}(\vec{r}_\perp^2 + \omega_{1j}^2)$, with $j = 0, 2$ and C_{1j}, ω_{1j}^2 some functions of α . Then, the integration over the perpendicular loop momentum can be readily performed since the integrand depends only on the square modulus of r_\perp (after dropping linear terms in the numerator since they vanish for symmetry). Adopting $d - 2$ dimensional spherical coordinates, the angular integration is trivial and the radial integral turns out to be of the form

$$\int_0^\infty d\rho \frac{\rho^{2n+1-2\epsilon}}{(\rho^2 + \omega_1^2)(\rho^2 + \omega_2^2)} = \frac{\pi}{2 \sin(\pi n - \pi\epsilon)} \frac{(\omega_1^2)^{n-\epsilon} - (\omega_2^2)^{n-\epsilon}}{\omega_1^2 - \omega_2^2} \quad \text{if} \quad -1 < n - \epsilon < 1 \quad (1.5)$$

where $n \in \{\mathbb{N}, 0\}$ and assuming $\omega_1^2, \omega_2^2 > 0$. Hence, within this framework, divergences are regulated through the dimension of the $d - 2$ dimensional perpendicular space. Lastly, the α integral can be evaluated by direct integration. Typically, one ends up with integrand terms of the general form $\alpha^a(\alpha - 1)^b(\eta\alpha - 1)^c$ which yields combinations of hyper-geometric and gamma functions. Interestingly, the gauge dependence through the parameter κ completely drops out in the end, leaving us with a gauge invariant expression. We therefore have the result

$$\frac{d\sigma_{\text{NLO,vir}}^{UUU}}{dx_B dy d\phi_l dz_h} = \frac{d\sigma_{\text{LO}}^{UUU}}{dx_B dy d\phi_l dz_h} \times \frac{\alpha_S}{2\pi} C_F S_\epsilon \left(\frac{\mu^2}{Q^2} \right)^\epsilon \left(-\frac{2}{\epsilon^2} - \frac{3}{\epsilon} - 8 \right) \quad (1.6)$$

with the common $\overline{\text{MS}}$ scheme constant $S_\epsilon = (4\pi)^\epsilon/\Gamma(1 - \epsilon)$. This in agreement with the original result for this γqq vertex correction [1].

In principle, we should also calculate two other diagrams, namely the self-energy corrections of the quark lines. Interestingly, if we repeat the very same procedure explained above, we find that after contour integration over β the denominator factor is proportional to r_\perp^2 only ($\omega_{ij}^2 = 0$) for both diagrams. This leads to a contribution that goes as

$$(\hat{\mathcal{M}}_{\text{NLO,vir,self-energy}}^{q \rightarrow q})^\rho \sim \int \frac{d^{d-2}r_\perp}{(2\pi)^{d-2}} \frac{A + B r_\perp^2}{r_\perp^2} \quad (1.7)$$

which vanishes. This is because, in dimensional regularization, it is consistent to set to zero all scale-less integrals [12]. Therefore, the vertex correction is the only virtual

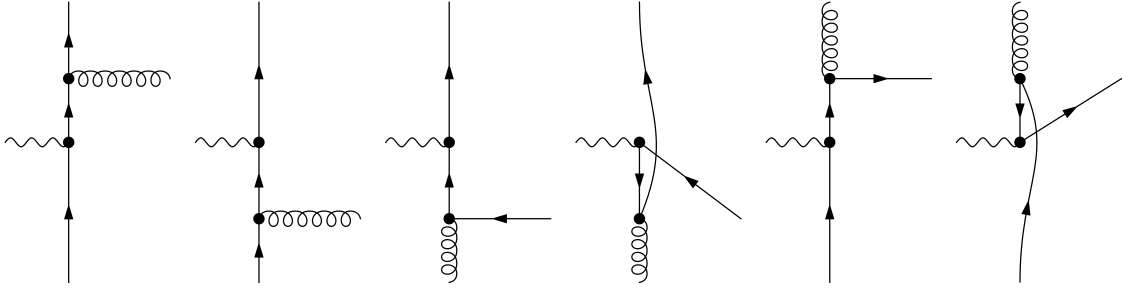


Figure 1.3: Real diagrams contributing to the leading-twist unpolarized cross section at NLO. All three partonic channels are shown: $q \rightarrow q$ channel (left), $g \rightarrow q$ channel (middle) and $q \rightarrow g$ channel (right).

diagram that has to be taken into account. Interestingly, this diagram leads to an hadronic tensor which is IR divergent only. No direct UV counterterms are then needed for this diagram (and for the two self-energy graphs, since they vanish). All in all, the full UV-renormalized virtual correction to the unpolarized cross section is just given by Eq. 1.6.

1.1.2 Real corrections

Another $\mathcal{O}(\alpha_S)$ correction to the cross section involves the emission of a final unobserved parton produced in the hard scattering process. At NLO, not only we can have the $q \rightarrow q$ channel (with real emission of gluons), but also $q \rightarrow g$ and $g \rightarrow q$ (with real emission of quarks). For all channels, the hadronic tensor is modified since there is an additional integration over the phase-space of the unobserved parton. The integrations in the hadronic tensors are modified according to

$$W_{\text{NLO,real}}^{\mu\nu} = \frac{e_a^2}{(2\pi)^{d-1}} \int d^d k \int d^d p \delta^+((q+k-p)^2) \text{Tr} \left[\hat{\mathcal{M}}_{\text{NLO}}^\mu \Phi^a \hat{\mathcal{M}}_{\text{NLO}}^\nu \Delta^a \right], \quad (1.8)$$

where the momentum r^μ of the unobserved parton is set to $r = q + k - p$. We work again in the Breit frame as before. Integration over dk^- and dp^+ is trivial. Here, since we are calculating the NLO corrections in the leading-twist unpolarized case, we can integrate over the transverse partonic momenta straight away. We are therefore left with integrations over the momentum fractions x and z . The delta function results in

the condition [10]

$$\delta^+((q+k-p)^2) = z z_h \delta \left(Q^2 z_h^2 \left(1 - \frac{z}{z_h} \right) \left(1 - \frac{x}{x_B} \right) - \vec{P}_{h\perp}^2 \right) \theta(q^0 + k^0 - p^0), \quad (1.9)$$

where the θ function restricts the kinematic variables in the following way

$$q^0 + k^0 - p^0 \geq 0 \iff \frac{x}{x_B} - \frac{z}{z_h} \left(1 + \frac{Q_T^2}{Q^2} \right) \geq 0 \iff \frac{x}{x_B} + \frac{z}{z_h} - 2 \geq 0. \quad (1.10)$$

Note that this condition would result in a complicated convolution of the x and z integrals due to the fact that the integration limits may depend on the other variable, i.e. the lower integration limits would result in either $z_{\min}(x)$ or $x_{\min}(z)$. However, one can greatly simplify the problem by simply ignoring the target fragmentation region, introducing a kinematical cut z_{cut} and x_{cut} [13]. In this work, we simply set the kinematical cut $z_{\text{cut}} \approx z_h$ and $x_{\text{cut}} \approx x_B$. With this prescription, the integration variables must satisfy $z > z_h$ and $x > x_B$ and our formulae match many results already available in the literature [4, 9]. We note however that one can also fully keep the integration limits x_{\min} and z_{\min} as they are, like done in [7]. Nothing really changes in the end, except for the fact that the integration limits are more complicated and numerically they would probably result in a slightly different overall value for the integrals.

The hadronic tensor now reads

$$W_{\mu\nu}^{\text{NLO,real}} = \frac{e_a^2 z_h}{(2\pi)^{d-1}} \int_{x_B}^1 dx \int_{z_h}^1 \frac{dz}{z} \delta \left(Q^2 z_h^2 \left(1 - \frac{z}{z_h} \right) \left(1 - \frac{x}{x_B} \right) - \vec{P}_{h\perp}^2 \right) w_{\mu\nu}, \quad (1.11)$$

where, depending on the channel, $w_{\mu\nu}$ assumes different forms

$$\begin{aligned} w_{\mu\nu}^{a,q \rightarrow q} &= \text{Tr} \left[\hat{\mathcal{M}}_{\mu}^{\text{NLO,real},q \rightarrow q} \Phi^a(x) \hat{\mathcal{M}}_{\nu}^{\text{NLO,real},q \rightarrow q} \Delta^a(z) \right], \\ w_{\mu\nu}^{a,g \rightarrow q} &= \Phi_g^{\lambda\eta}(x) \text{Tr} \left[\hat{\mathcal{M}}_{\mu\lambda}^{\text{NLO,real},g \rightarrow q} \hat{\mathcal{M}}_{\nu\eta}^{\text{NLO,real},g \rightarrow q} \Delta^a(z) \right], \\ w_{\mu\nu}^{a,q \rightarrow g} &= \Delta_g^{\lambda\eta}(z) \text{Tr} \left[\hat{\mathcal{M}}_{\mu\lambda}^{\text{NLO,real},q \rightarrow g} \Phi^a(x) \hat{\mathcal{M}}_{\nu\eta}^{\text{NLO,real},q \rightarrow g} \right], \end{aligned} \quad (1.12)$$

where $\Phi_g^{\mu\nu}(x)$ and $\Delta_g^{\mu\nu}(z)$ are the gluon distribution and fragmentation correlators respectively. Next, the phase-space integration over the transverse momentum of the detected hadron can be performed by using symmetry, switching to $d-2$ dimensional spherical coordinates and making use of the delta function. Also, for further manipu-

lation, it is convenient and common to work with scaled variables defined as $w \equiv x_B/x$ and $v \equiv z_h/z$. The $P_{h\perp}$ -integrated hadronic tensor then is

$$\begin{aligned} \int d^{d-2} P_{h\perp} W_{\mu\nu}^{\text{NLO,real}} &= \frac{e_a^2 z_h^{1-2\epsilon} x_B}{Q^{2\epsilon} 8\pi^2} S_\epsilon \int_{x_B}^1 \frac{dw}{w} \int_{z_h}^1 \frac{dv}{v} \frac{1}{w} \\ &\times \left(\frac{v-1}{v} \right)^{-\epsilon} \left(\frac{w-1}{w} \right)^{-\epsilon} w_{\mu\nu}^a \Big|_{\chi_T^2 = (1-\frac{1}{v})(1-\frac{1}{w})}. \end{aligned} \quad (1.13)$$

Evidently the integral is not well-behaved for $w, v \rightarrow 1$, since it contains non-integrable functions of w and v . In order to work with well-behaved quantities and extract the singular behavior of the integral we do the following. After performing the Dirac trace, denoting f and D generic PDFs and FFs respectively, we can write the integrated hadronic tensor in the form

$$\int d^{d-2} P_{h\perp} W_{\mu\nu}^{\text{NLO,real}} = \int_{x_B}^1 dw \int_{z_h}^1 dv \frac{\hat{\mathcal{W}}_{\mu\nu}(w, v)}{(1-w)^{1+\epsilon}(1-v)^{1+\epsilon}} f(x_B/w) D(z_h/v), \quad (1.14)$$

where $\hat{\mathcal{W}}(w, v)$ is finite in the limit $w, v \rightarrow 1$. This re-writing of the integrand allows us to extract the $1/\epsilon$ poles and make them manifest in our expressions. This is because we can now use the useful distribution relation [12]

$$\frac{1}{(1-w)^{1+\epsilon}} = -\frac{1}{\epsilon} \delta(1-w) + \frac{1}{(1-w)_+} - \epsilon \left(\frac{\ln(1-w)}{1-w} \right)_+ + \mathcal{O}(\epsilon^2), \quad (1.15)$$

where the $+$ prescription is defined by [14]

$$\int_{x_B}^1 dw h(w) \left(\frac{g(w)}{1-w} \right)_+ = \int_{x_B}^1 dw \frac{h(w) - h(1)}{1-w} g(w) - h(1) \int_0^{x_B} dw \frac{g(w)}{1-w}. \quad (1.16)$$

Naturally, these distributional identities are analogous for v as well. This procedure makes the $1/\epsilon$ poles explicit and leads to the well-known cancellation of infrared singularities between real and virtual contributions (commonly referred as infrared safety [8]). We do indeed observe this cancellation of $1/\epsilon^2$ poles in our calculation. However, the partonic cross section typically still exhibits collinear singularities emerging when the parton (coming from the nucleon or fragmenting) becomes collinear with the unobserved parton [6]. The standard procedure is to absorb these collinear poles into $\overline{\text{MS}}$ -renormalized parton distribution and fragmentation functions [1, 3]. The corresponding

poles can be removed in the $\overline{\text{MS}}$ scheme by introducing renormalized functions

$$\begin{aligned} f_{\text{bare}}^q(x, \mu) &= f_{\text{ren}}^q(x, \mu) + \frac{\alpha_S}{2\pi} \frac{S_\epsilon}{\epsilon} [P_{qq} \otimes f_{\text{ren}}^q + P_{qg} \otimes f_{\text{ren}}^g](x, \mu) \\ D_{\text{bare}}^q(z, \mu) &= D_{\text{ren}}^q(z, \mu) + \frac{\alpha_S}{2\pi} \frac{S_\epsilon}{\epsilon} [P_{qq} \otimes D_{\text{ren}}^q + P_{gq} \otimes D_{\text{ren}}^g](z, \mu) \end{aligned} \quad (1.17)$$

with splitting functions

$$\begin{aligned} P_{qq}(y) &= C_F \left[\frac{1+y^2}{(1-y)_+} + \frac{3}{2} \delta(1-y) \right] \\ P_{qg}(y) &= T_F [y^2 + (1-y)^2] \\ P_{gq}(y) &= C_F \left[\frac{1+(1-y)^2}{y} \right] \end{aligned} \quad (1.18)$$

where the convolution \otimes is a short-hand for

$$(P \otimes f)(x) \equiv \int_x^1 \frac{dy}{y} P(y) f\left(\frac{x}{y}\right) \quad (1.19)$$

With such splitting functions, inserting the bare distributions into the LO expression for the cross section leads to additional terms that precisely cancel the collinear poles associated with the observed partons in the NLO partonic cross section.

We obtain the following unpolarized NLO result, which is consistent with the literature [4]

$$\begin{aligned} \frac{d\sigma_{\text{LO+NLO}}^{UUU}}{dx_B dy d\phi_l dz_h} &= \frac{2\alpha_{\text{em}}^2}{yQ^2} \left[\left(1-y+\frac{y^2}{2}\right) \mathcal{F}_{UU,T} + (1-y) \mathcal{F}_{UU,L} \right] \\ \mathcal{F}_{UU,T}(x_B, z_h, Q^2) &= \sum_a e_a^2 \left(f_1^a \circ \mathcal{C}_U^{a \rightarrow a} \circ D_1^a + f_1^g \circ \mathcal{C}_U^{g \rightarrow a} \circ D_1^a + f_1^a \circ \mathcal{C}_U^{a \rightarrow g} \circ D_1^g \right) \\ \mathcal{F}_{UU,L}(x_B, z_h, Q^2) &= \sum_a e_a^2 \left(f_1^a \circ \mathcal{C}_L^{a \rightarrow a} \circ D_1^a + f_1^g \circ \mathcal{C}_L^{g \rightarrow a} \circ D_1^a + f_1^a \circ \mathcal{C}_L^{a \rightarrow g} \circ D_1^g \right) \end{aligned} \quad (1.20)$$

where we introduced the convolution \circ defined as

$$f \circ \mathcal{C} \circ D = \int_{x_B}^1 \frac{dw}{w} \int_{z_h}^1 \frac{dv}{v} f\left(\frac{x_B}{w}\right) \mathcal{C}(w, v) D\left(\frac{z_h}{v}\right) \quad (1.21)$$

The functions \mathcal{C}_U and \mathcal{C}_L are the unpolarized NLO hard-scattering coefficients relative to the unpolarized structure functions $F_{UU,U}$ and $F_{UU,L}$ respectively [2]. It is very interesting to note that the unpolarized structure function $F_{UU,L}$ is populated at NLO, while it is zero at LO. The coefficients \mathcal{C}_U and \mathcal{C}_L are given by

$$\begin{aligned}
 \mathcal{C}_U^{a \rightarrow a}(w, v) &= \left[1 + \frac{\alpha_S(\mu)}{2\pi} C_F \left(-8 - 3 \ln \frac{\mu^2}{Q^2} \right) \right] \delta(1-w) \delta(1-v) \\
 &+ \frac{\alpha_S(\mu)}{2\pi} C_F \left[(1+v^2) \left(\frac{\ln(1-v)}{1-v} \right)_+ + 1-v + (1+v^2) \frac{\ln v - \ln \frac{\mu^2}{Q^2}}{(1-v)_+} \right] \delta(1-w) \\
 &+ \frac{\alpha_S(\mu)}{2\pi} C_F \left[(1+w^2) \left(\frac{\ln(1-w)}{1-w} \right)_+ + 1-w + (1+w^2) \frac{-\ln w - \ln \frac{\mu^2}{Q^2}}{(1-w)_+} \right] \delta(1-v) \\
 &+ \frac{\alpha_S(\mu)}{2\pi} C_F \left[\frac{2v^2w^2 - 2v^2w - 2vw^2 + 4vw + v^2 + w^2 - 2v - 2w + 2}{(1-w)_+(1-v)_+} \right] \\
 \mathcal{C}_U^{g \rightarrow a}(w, v) &= \frac{\alpha_S(\mu)}{2\pi} T_F \left[(w^2 + (1-w)^2) \left(\ln \frac{1-w}{w} - \ln \frac{\mu^2}{Q^2} \right) + 2w(1-w) \right] \delta(1-v) \\
 &+ \frac{\alpha_S(\mu)}{2\pi} T_F \left[\frac{(w^2 + (1-w)^2)(v^2 + (1-v)^2)}{v(1-v)_+} \right] \\
 \mathcal{C}_U^{a \rightarrow g}(w, v) &= \frac{\alpha_S(\mu)}{2\pi} C_F \left[\frac{1 + (1-v)^2}{v} \left(\ln(v(1-v)) - \ln \frac{\mu^2}{Q^2} \right) + v \right] \delta(1-w) \\
 &+ \frac{\alpha_S(\mu)}{2\pi} C_F \left[\frac{1 + v^2 + w^2 - 2vw^2 - 2v^2w + 2v^2w^2}{v(1-w)_+} \right]
 \end{aligned} \tag{1.22}$$

and

$$\begin{aligned}
 \mathcal{C}_L^{a \rightarrow a}(w, v) &= \frac{\alpha_S(\mu)}{2\pi} C_F [4vw] \\
 \mathcal{C}_L^{g \rightarrow a}(w, v) &= \frac{\alpha_S(\mu)}{2\pi} T_F [8w(1-w)] \\
 \mathcal{C}_L^{a \rightarrow g}(w, v) &= \frac{\alpha_S(\mu)}{2\pi} C_F [4w(1-v)]
 \end{aligned} \tag{1.23}$$

1.2 Transverse nucleon spin

We now turn our attention to the case of transversely-polarized protons. As already shown at LO (REF), the spin-dependent cross section can be obtained within the

collinear twist-3 formalism. Here, we will derive the NLO corrections contributing to the A_{UTU} spin asymmetry. Evidently, the complexity of the calculation increases significantly compared to the unpolarized case. In the literature there are very few similar NLO calculations for SIDIS, and they mostly focus on the $P_{h\perp}$ -weighed asymmetries (ADD LIT). This being said, the NLO methodologies presented in the previous section can be directly generalized to this higher-twist case, provided we take into account the additional structures of twist-3 correlators and handle the relative hard parts with care. As far as this work goes, we will restrict ourselves to the case of the qq and qqq fragmentation channels. This already provides good insights into how a twist-3 NLO calculation can be performed, and it is an important reference for similar future work. (HERE OVERALL RESULTS: IR safety, gauge invariance, etc...)

1.2.1 Virtual graphs

Let us start with the virtual corrections. The NLO diagrams contributing at the twist-3 level are identical to the unpolarized case, when it comes to intrinsic and kinematical contributions (see Fig. 1.1). For those terms, we employ the same methods as in the leading-twist NLO case but with different correlators structures. For dynamical twist-3 though, there are more diagrams that have to be taken into account. The dynamical twist-3 diagrams relevant at NLO are shown in Fig. 1.4. As before, we write the loop momenta in their light-cone decomposition $d^d r = d\alpha d^{d-2} r_\perp d\beta$ and perform contour integration over the longitudinal momentum fraction β . Next, the transverse components are integrated out in $d - 2$ dimensions. Lastly, the integral over the longitudinal momentum fraction α is performed. Similarly to the unpolarized case, we find that self-energy diagrams for external quark and gluon lines vanish (diagrams a, c, d, e and f), since they are given by massless integrals. We are therefore left with seven diagrams: the self-energy graph b , the vertex corrections g, h, i and the box diagrams j, k and l . As pointed out already, treating gluons in light-cone gauge is advantageous within the twist-3 formalism. In fact, not only we can easily derive a factorization formula at sub-leading twist, but also the gauge invariance of partonic cross sections can be tested throughout the calculation. By writing the polarization sum for gluons as

$$\sum_{\lambda=\pm 1} \epsilon_\lambda^\mu(r) \epsilon_\lambda^{\nu*}(r) = -g^{\mu\nu} + \kappa \frac{r^\mu m^\nu + r^\nu m^\mu}{r \cdot m}, \quad (1.24)$$

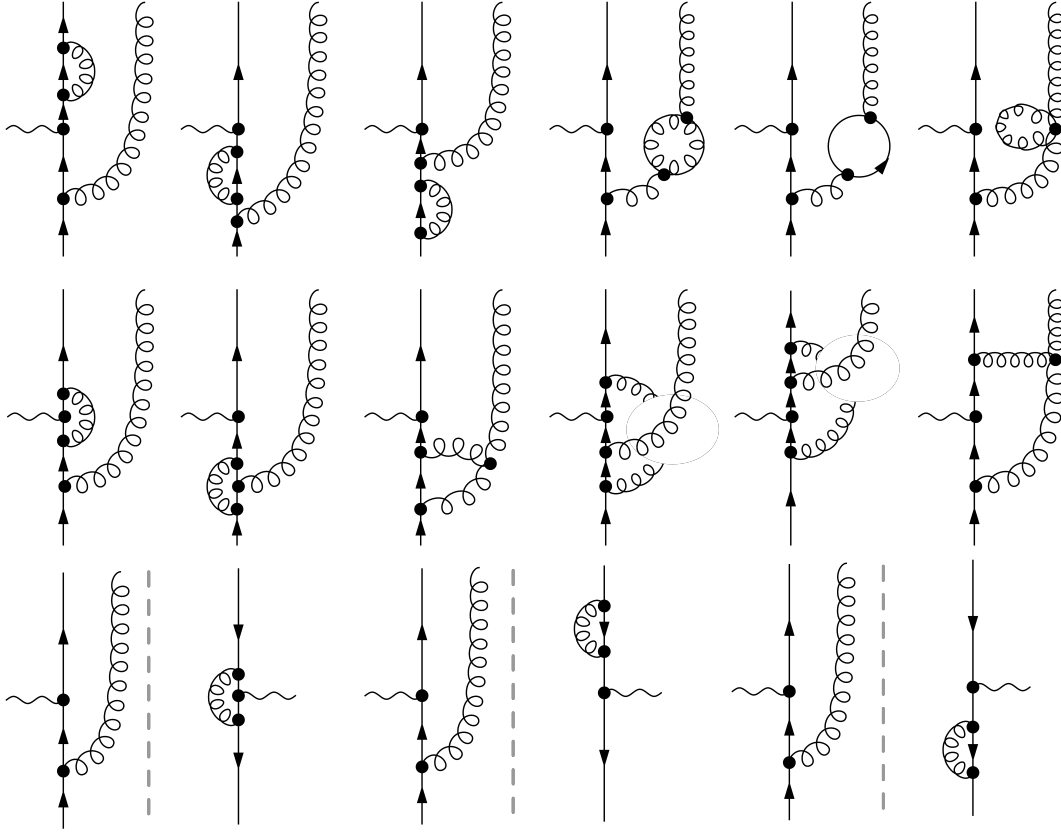


Figure 1.4: Virtual diagrams contributing to the NLO dynamical twist-3 qg fragmentation channel.

we can easily check that if gauge parameter κ drops out of the final result, as it should, proving the gauge invariance of the cross section. For virtual graphs, we find that gauge invariance is restored only when all the diagrams in Fig. 1.4 are added, since individual diagrams depend on κ . We will later show that gauge invariance for real graphs is less obvious, since it requires all twist-3 contributions and the use of the equation of motion relations presented in Sec. REF.

1.2.2 Real graphs

We now move on to the case of real radiation. Focusing on the qg fragmentation channel, there can only be emission of gluons. Hence, real NLO corrections in the twist-3 case

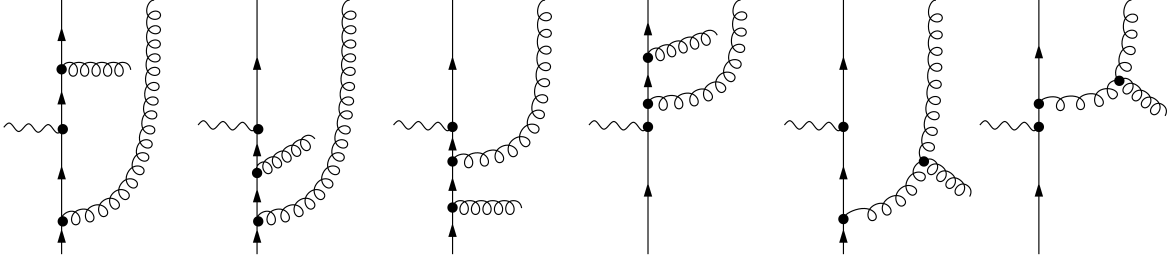


Figure 1.5: Real diagrams contributing to the NLO dynamical twist-3 qq fragmentation channel. Each of these diagrams interferes with the two leading-twist real $q \rightarrow q$ NLO corrections in Fig. 1.3.

are simply obtained by adding gluon lines to LO twist-3 fragmentation diagrams. The relevant diagrams are shown in Fig. 1.5.

Bibliography

- [1] G. Altarelli, R.K. Ellis, and G. Martinelli. “Large perturbative corrections to the Drell-Yan process in QCD”. en. In: *Nuclear Physics B* 157.3 (Oct. 1979), pp. 461–497. ISSN: 05503213. DOI: 10.1016/0550-3213(79)90116-0. URL: <https://linkinghub.elsevier.com/retrieve/pii/0550321379901160> (visited on 02/13/2025).
- [2] Alessandro Bacchetta et al. “Semi-inclusive deep inelastic scattering at small transverse momentum”. en. In: *Journal of High Energy Physics* 2007.02 (Feb. 2007). arXiv:hep-ph/0611265, pp. 093–093. ISSN: 1029-8479. DOI: 10.1088/1126-6708/2007/02/093. URL: <http://arxiv.org/abs/hep-ph/0611265> (visited on 02/07/2025).
- [3] John Collins. *Foundations of Perturbative QCD*. Cambridge Monographs on Particle Physics, Nuclear Physics and Cosmology. Cambridge University Press, 2011.
- [4] D. de Florian, M. Stratmann, and W. Vogelsang. “QCD analysis of unpolarized and polarized Λ -baryon production in leading and next-to-leading order”. In: *Physical Review D* 57.9 (May 1998), 5811–5824. ISSN: 1089-4918. DOI: 10.1103/PhysRevD.57.5811. URL: <http://dx.doi.org/10.1103/PhysRevD.57.5811>.
- [5] Daniel de Florian, Rodolfo Sassot, and Marco Stratmann. “Global analysis of fragmentation functions for protons and charged hadrons”. In: *Physical Review D* 76.7 (Oct. 2007). ISSN: 1550-2368. DOI: 10.1103/PhysRevD.76.074033. URL: <http://dx.doi.org/10.1103/PhysRevD.76.074033>.
- [6] Patriz Hinderer, Marc Schlegel, and Werner Vogelsang. “Single-Inclusive Production of Hadrons and Jets in Lepton-Nucleon Scattering at NLO”. en. In: *Physical Review D* 92.1 (July 2015). arXiv:1505.06415 [hep-ph], p. 014001. ISSN: 1550-7998, 1550-2368. DOI: 10.1103/PhysRevD.92.014001. URL: <http://arxiv.org/abs/1505.06415> (visited on 02/06/2025).

- [7] Koichi Kanazawa and Yuji Koike. “Contribution of the twist-3 fragmentation function to the single transverse-spin asymmetry in semi-inclusive deep inelastic scattering”. en. In: *Physical Review D* 88.7 (Oct. 2013), p. 074022. ISSN: 1550-7998, 1550-2368. DOI: 10.1103/PhysRevD.88.074022. URL: <https://link.aps.org/doi/10.1103/PhysRevD.88.074022> (visited on 02/06/2025).
- [8] Toichiro Kinoshita. “Mass Singularities of Feynman Amplitudes”. In: *Journal of Mathematical Physics* 3.4 (July 1962). eprint: https://pubs.aip.org/aip/jmp/article-pdf/3/4/650/19167464/650_1_online.pdf, pp. 650–677. ISSN: 0022-2488. DOI: 10.1063/1.1724268. URL: <https://doi.org/10.1063/1.1724268>.
- [9] Yuji Koike, Junji Nagashima, and Werner Vogelsang. “Resummation for polarized semi-inclusive deep-inelastic scattering at small transverse momentum”. In: *Nuclear Physics B* 744.1–2 (June 2006), 59–79. ISSN: 0550-3213. DOI: 10.1016/j.nuclphysb.2006.03.009. URL: <http://dx.doi.org/10.1016/j.nuclphysb.2006.03.009>.
- [10] Yuji Koike et al. “Transverse Polarization of Hyperons Produced in Semi-Inclusive Deep Inelastic Scattering”. en. In: *Physical Review D* 105.5 (Mar. 2022). arXiv:2202.00338 [hep-ph], p. 056021. ISSN: 2470-0010, 2470-0029. DOI: 10.1103/PhysRevD.105.056021. URL: <http://arxiv.org/abs/2202.00338> (visited on 02/06/2025).
- [11] A. D. Martin et al. “Parton distributions for the LHC”. In: *The European Physical Journal C* 63.2 (July 2009), 189–285. ISSN: 1434-6052. DOI: 10.1140/epjc/s10052-009-1072-5. URL: <http://dx.doi.org/10.1140/epjc/s10052-009-1072-5>.
- [12] Matthew D. Schwartz. *Quantum Field Theory and the Standard Model*. Cambridge University Press, Mar. 2014.
- [13] A. N. Sissakian, O. Yu. Shevchenko, and O. N. Ivanov. “NLO QCD procedure of the semi-inclusive deep inelastic scattering data analysis with respect to the light quark polarized sea”. In: *Physical Review D* 70.7 (Oct. 2004). ISSN: 1550-2368. DOI: 10.1103/physrevd.70.074032. URL: <http://dx.doi.org/10.1103/PhysRevD.70.074032>.
- [14] George Sterman et al. “Handbook of perturbative QCD”. In: *Rev. Mod. Phys.* 67 (1 Jan. 1995), pp. 157–248. DOI: 10.1103/RevModPhys.67.157. URL: <https://link.aps.org/doi/10.1103/RevModPhys.67.157>.